The EMBO Journal (2006) 25, 80–87 | © 2006 European Molecular Biology Organization | All Rights Reserved 0261-4189/06
www.embojournal.org

THE EMBO JOURNAL

Structural basis for Gas6–Axl signalling

Takako Sasaki[1], Pjotr G Knyazev[1], Naomi J Clout[2], Yuri Cheburkin[1], Walter Göhring[1], Axel Ullrich[1], Rupert Timpl[1] and Erhard Hohenester[2,*]

[1]Max-Planck-Institut für Biochemie, Martinsried, Germany and [2]Division of Cell and Molecular Biology, Imperial College London, London, UK

Receptor tyrosine kinases of the Axl family are activated by the vitamin K-dependent protein Gas6. Axl signalling plays important roles in cancer, spermatogenesis, immunity, and platelet function. The crystal structure at 3.3 Å resolution of a minimal human Gas6/Axl complex reveals an assembly of 2:2 stoichiometry, in which the two immunoglobulin-like domains of the Axl ectodomain are crosslinked by the first laminin G-like domain of Gas6, with no direct Axl/Axl or Gas6/Gas6 contacts. There are two distinct Gas6/Axl contacts of very different size, both featuring interactions between edge β-strands. Structure-based mutagenesis, protein binding assays and receptor activation experiments demonstrate that both the major and minor Gas6 binding sites are required for productive transmembrane signalling. Gas6-mediated Axl dimerisation is likely to occur in two steps, with a high-affinity 1:1 Gas6/Axl complex forming first. Only the minor Gas6 binding site is highly conserved in the other Axl family receptors, Sky/Tyro3 and Mer. Specificity at the major contact is suggested to result from the segregation of charged and apolar residues to opposite faces of the newly formed β-sheet.

The EMBO Journal (2006) **25,** 80–87. doi:10.1038/sj.emboj.7600912; Published online 15 December 2005
Subject Categories: signal transduction; structural biology
Keywords: immunoglobulin-like domain; laminin G-like domain; receptor tyrosine kinase; site-directed mutagenesis; X-ray crystallography

Introduction

Receptor tyrosine kinases (RTKs) play critical roles in the control of many cellular processes, such as the cell cycle, cell metabolism and survival, proliferation and differentiation, and cell migration (reviewed in Schlessinger, 2000; Gschwind *et al*, 2004). The prototypical RTKs are activated by growth factors, which promote receptor dimerisation and, in turn, autophosphorylation of tyrosine residues within the cytosolic domain. Binding of signalling proteins to these phosphorylated tyrosine residues then leads to downstream signalling. Axl and its homologues, Sky/Tyro3 and Mer, constitute an RTK subfamily characterised by an extracellular domain resembling cell adhesion molecules, consisting of two immunoglobulin-like (IG) domains followed by two fibronectin type 3-like domains (Janssen *et al*, 1991; O'Bryan *et al*, 1991; Rescigno *et al*, 1991). Axl family RTKs are unique in that they are activated by Gas6, a member of the vitamin K-dependent protein family that resembles blood coagulation factors rather than typical growth factors (Ohashi *et al*, 1995; Stitt *et al*, 1995; Varnum *et al*, 1995; Mark *et al*, 1996). Gas6 consists of a γ-carboxyglutamate (Gla)-rich domain that mediates binding to phospholipid membranes, four epidermal growth factor-like domains, and two laminin G-like (LG) domains (Manfioletti *et al*, 1993). Gas6 is ∼40% identical to protein S, a negative regulator of blood coagulation that can also activate Axl RTKs under certain nonphysiological conditions (Godowski *et al*, 1995).

The biological consequences of Axl activation are complex. Axl was initially identified as a transforming gene product (Janssen *et al*, 1991; O'Bryan *et al*, 1991), and Axl expression is indeed upregulated in human tumours (Nakano *et al*, 2003; Sun *et al*, 2004). Many studies have shown that Gas6–Axl signalling promotes cell survival and growth *in vitro* (e.g. Nakano *et al*, 1995; Goruppi *et al*, 1996; Li *et al*, 1996; O'Donnell *et al*, 1999; Shankar *et al*, 2003). Recent gene knockout studies have revealed fundamental roles of Axl RTKs in spermatogenesis (Lu *et al*, 1999), immunity (Lu and Lemke, 2001; Scott *et al*, 2001), platelet function (Angelillo-Scherrer *et al*, 2001, 2005) and kidney pathology (Yanagita *et al*, 2002). The role of Gas6–Axl signalling in platelets is particularly interesting. Cross-talk between Axl RTKs and $\alpha_{IIb}\beta_3$ integrin, via PI3 kinase and Akt, contributes to platelet activation and thrombus stabilisation. Importantly, blocking of Gas6–Axl signalling in mice prevents thrombosis without causing the bleeding side effects that blight other antithrombotic therapies (Angelillo-Scherrer *et al*, 2005; Gould *et al*, 2005). A better understanding of the molecular recognition events leading to Axl activation is thus of considerable interest.

Previous studies have shown that the Axl binding site of Gas6 is fully contained within the C-terminal LG domain pair (Gas6-LG) (Mark *et al*, 1996; Tanabe *et al*, 1997). A structure determination of Gas6-LG revealed a V-shaped arrangement of two canonical LG domains, reinforced by an interdomain calcium binding site (Sasaki *et al*, 2002). Like in the related LG pair of the laminin α2 chain (Tisi *et al*, 2000), the N-terminal segment of Gas6-LG is disulfide-bonded to the second LG domain, LG2. A hydrophobic patch on LG2 was tentatively assigned as an Axl binding region, but how Gas6 binds to and activates Axl remained unclear (Sasaki *et al*, 2002). A recent structure determination of the IG domains of Sky also failed to give insight into this critical question (Heiring *et al*, 2004). Here we report the crystal structure and mutational analysis of a minimal Gas6/Axl complex. Our results demonstrate that Gas6 initiates signalling by

*Corresponding author. Biophysics Section, Blackett Laboratory, Imperial College London, London SW7 2AZ, UK.
Tel.: +44 20 7594 7701; Fax +44 20 7589 0191;
E-mail: e.hohenester@imperial.ac.uk

Received: 2 September 2005; accepted: 21 November 2005; published online: 15 December 2005

crosslinking its receptor by an unusual mechanism of β-sheet juxtaposition. The Gas6/Axl structure provides a framework for future functional studies and should be useful in developing reagents blocking aberrant Axl signalling in human diseases.

Results

Overall structure of the minimal Gas6–Axl complex

The soluble Axl ectodomain binds Gas6-LG with nanomolar affinity (Sasaki *et al*, 2002) and 1:1 stoichiometry, as determined by analytical ultracentrifugation (data not shown). We found that an Axl fragment spanning the two N-terminal IG domains and lacking carbohydrate modifications (Axl-IG) retains full Gas6-LG binding activity. We crystallised the human Gas6-LG/Axl-IG complex and have determined its structure at 3.3 Å resolution ($R_{free} = 0.265$). The asymmetric unit of the crystals contains a symmetric 2:2 Gas6-LG/Axl-IG assembly, in which the Axl-IG molecules are located on the outside and are linked by two Gas6-LG molecules (Figure 1). There are no direct ligand/ligand or receptor/receptor contacts. Only LG1 of Gas6 is involved in Axl binding, whereas both IG1 and IG2 of Axl are involved in Gas6 binding. The three predicted glycosylation sites of Axl-IG ($Asn36^{Axl}$, $Asn150^{Axl}$ and $Asn191^{Axl}$) are distant from the Gas6-LG molecules in the 2:2 complex, consistent with our finding that Axl glycosylation has no influence on high-affinity Gas6 binding.

Structure of Gas6-LG and Axl-IG in the complex

The structure of Gas6-LG in the complex is very similar to that of free Gas6-LG (Sasaki *et al*, 2002), but there is a small reorientation by 9° in the interdomain angle, and two previously disordered segments in $LG1^{Gas6}$ become ordered upon complex formation (see below). The two IG domains of Axl-IG are arranged in a fully extended fashion that differs from the bent conformation seen in the IG pair of the homologous receptor, Sky (Heiring *et al*, 2004) (Figure 2). $IG1^{Axl}$ belongs to the intermediate (I) set of the IG superfamily, with the two β-sheets showing the characteristic ABED and A′GFCC′ topology (Chothia and Jones, 1997). The putative glycosylation site at $Asn36^{Axl}$ is located in strand A′. $IG2^{Axl}$ also resembles the I set, but strand D is missing, similar to the situation in ICAM-1 (Casasnovas *et al*, 1998). Putative glycosylation sites are located in strand B ($Asn150^{Axl}$) and the E-F loop ($Asn191^{Axl}$). A comparison of the Axl and Sky structures reveals remarkable differences in their IG1 domains (r.m.s. deviation 2.4 Å for 79 Cα atoms; Figure 2B), whereas their IG2 domains are quite similar (r.m.s. deviation 0.74 Å for 78 Cα atoms). IG1 of Sky deviates from $IG1^{Axl}$ and all other I-set members, in that strand G (rather than strand A) switches between the two β-sheets of the domain, hydrogen bonding first to strand B and then to strand F (Heiring *et al*, 2004). Another notable difference is that the IG pair of Sky is dimeric, with the ABED sheet of the IG1 domain forming the dimer interface (discussed below).

Two types of Gas6/Axl contacts

There are two distinct ligand/receptor contacts in the 2:2 Gas6-LG/Axl-IG complex described here. The major contact, between $LG1^{Gas6}$ and $IG1^{Axl}$, buries 2366 $Å^2$ of solvent-accessible surface area and, given its size, is tentatively assigned as the high-affinity interaction site (confirmed below). The minor contact, between $LG1^{Gas6}$ and $IG2^{Axl}$, buries 765 $Å^2$. Remarkably, both types of contact feature the juxtaposition of edge β-strands, so that continuous β-sheets are formed across both Gas6/Axl contacts (Figure 1C). Neither contact displays particularly good shape complementarity: when evaluated with the program SC (CCP4-Collaborative Computing Project No. 4, 1994), the major contact scores 0.54, and the minor contact 0.63 (a score of 1 indicating perfect complementarity of the interacting surfaces). In the crystal lattice, Gas6-LG/Axl-IG complexes are arranged in infinite linear arrays, with a two-fold noncrystallographic symmetry axis producing an

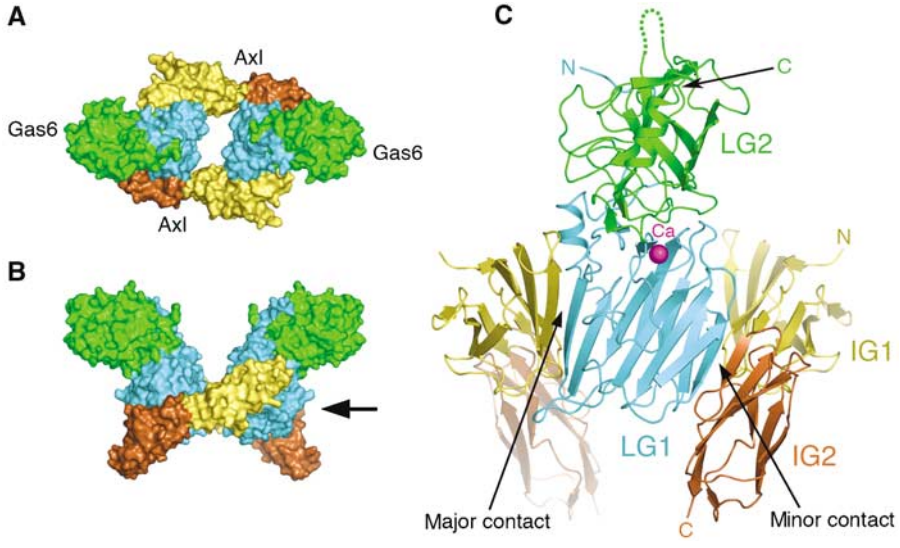

Figure 1 Overall architecture of the Gas6-LG/Axl-IG complex. Shown are three orthogonal views. (**A**) Top view, towards the cell membrane harbouring the receptor. (**B**) Side view, with the cell membrane at the bottom. (**C**) Front view, in the direction indicated by the arrow in (B). Surface representations are shown in (A) and (B), while a cartoon representation is shown in (C). Gas6-LG is in cyan (N-terminal segment and LG1) and green (LG2), Axl-IG is in yellow (IG1) and brown (IG2). In (C), the Gas6-LG molecule at the back has been removed for clarity, a calcium ion in the LG1–LG2 interface is shown as a pink sphere, and the Gas6/Axl contact sites are labelled.

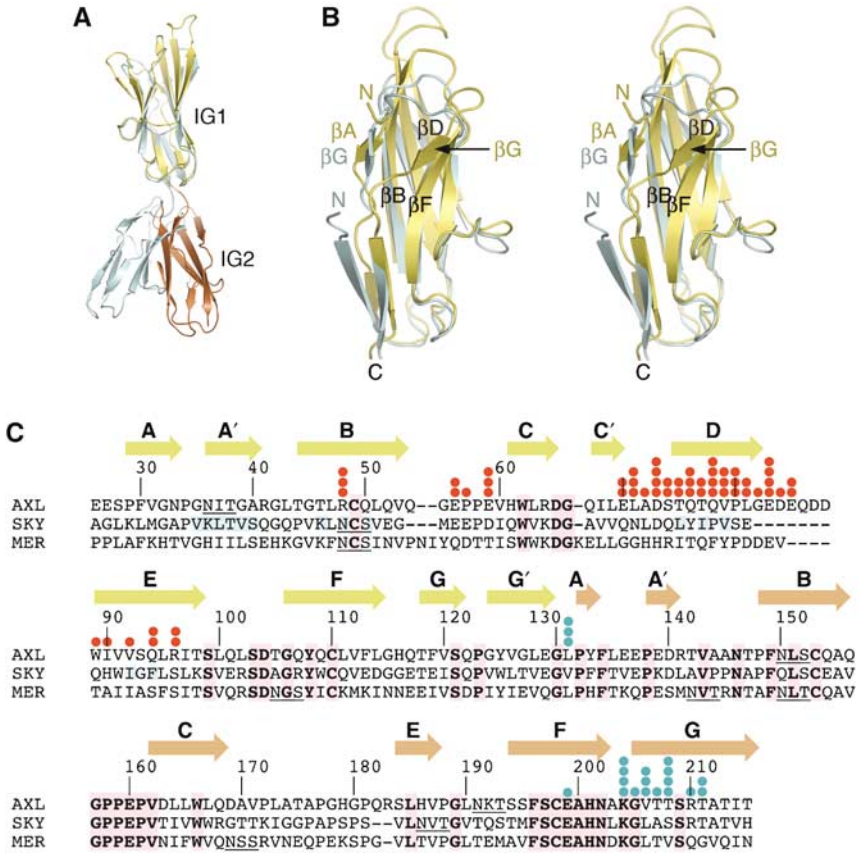

Figure 2 Comparison of Axl family members. (**A**) Comparison of the structures of Axl-IG (this work) and a Sky-IG monomer (Heiring *et al*, 2004). The two structures were superimposed using their IG1 domains. Axl is shown in yellow (IG1) and brown (IG2), Sky in light blue. (**B**) Stereoview showing a superposition of the IG1 domains of Axl and Sky (r.m.s. deviation 2.4 Å for 79 Cα atoms). The colouring scheme is the same as in (A), but the view direction is different. The polypeptide chain termini and selected β-strands are labelled. Strand G of Sky occupies the position of strand A of Axl. The major Gas6 binding site is located in strand D at the back. (**C**) Sequence alignment of human Axl, Sky and Mer. The alignment of Axl and Sky is based on their structural superposition; the Mer sequence was aligned manually to maximise conservation of structurally important residues. The Axl numbering scheme and location of β-strands are indicated above the alignment. Conserved residues are in bold and shaded pink. Axl residues involved in the major and minor Gas6 binding sites are marked, respectively, by red and cyan filled circles above the alignment. The number of circles is proportional to the surface area buried upon complex formation with Gas6: one circle, 10–30 Å^2; two circles, 30–50 Å^2; three circle, 50–70 Å^2; four circles, >70 Å^2. Sky residues involved in dimer formation (Heiring *et al*, 2004) are shaded light blue. Predicted Asn-linked glycosylation sites are underlined.

Axl/Axl contact that buries 2×814 Å^2 of solvent-accessible surface (SC score 0.48). The resulting 'Axl dimer' does not resemble the much tighter Sky dimer (Heiring *et al*, 2004) and is probably nonphysiological, given the paucity of specific interactions and the presence of Ni^{2+} ions in the interface (Supplementary Figure S1).

Major Gas6/Axl contact

The core of the major Gas6/Axl contact is formed by the antiparallel interaction of strand B of LG1^{Gas6} and strand D of IG1^{Axl} (six main-chain hydrogen bonds). Formation of a continuous β-sheet across the major Gas6/Axl contact leads to a striking segregation of charged and apolar residues. On one face of the β-sheet, an extensive network of charged residues is formed, with Arg308^{Gas6}, Arg310^{Gas6} and Lys312^{Gas6} interacting with Glu56^{Axl} and Glu59^{Axl}; the latter two residues are contributed by the B-C loop located above strand D of IG1^{Axl} (Figure 3A). The two *N*-acetylglucosamine moieties attached to Asn420^{Gas6} pack against Arg310^{Gas6} and are close to Axl, but appear to make no specific interactions with the receptor. The opposite face of the major contact is devoid of charged residues and is dominated by apolar interactions, most prominently between Thr75^{Axl}, Thr77^{Axl}, Val79^{Axl}, Ile90^{Axl} and Val92^{Axl} on the one hand, and Ile307^{Gas6}, Leu309^{Gas6}, Phe311^{Gas6}, Thr457^{Gas6}, Ile458^{Gas6}, Thr461^{Gas6} and Met468^{Gas6} on the other hand (Figure 3B). Gas6 residues 457–464 are part of a short α-helix that was not seen in free Gas6-LG (Sasaki *et al*, 2002). This helix therefore appears to become ordered only upon receptor binding, although its association with Axl is remarkably loose (there are only two van der Waals contacts closer than 4 Å). Finally, the A–B loop in LG1^{Gas6} is also disordered in free Gas6-LG, but contributes two Axl-binding residues, Arg299^{Gas6} and Ser302^{Gas6}, in the complex.

We previously reported that mutation of Leu620^{Gas6} and Tyr660^{Gas6} in LG2^{Gas6} has a modest effect on Axl binding and activation (Sasaki *et al*, 2002), yet we now see that LG2^{Gas6} is not directly involved in receptor binding. However, Leu620^{Gas6} and Tyr660^{Gas6} are close to the Axl-binding A-B loop in LG1^{Gas6} (12 and 3.5 Å, respectively), suggesting that their mutation may have affected the Gas6/Axl interaction at the major site in an indirect manner.

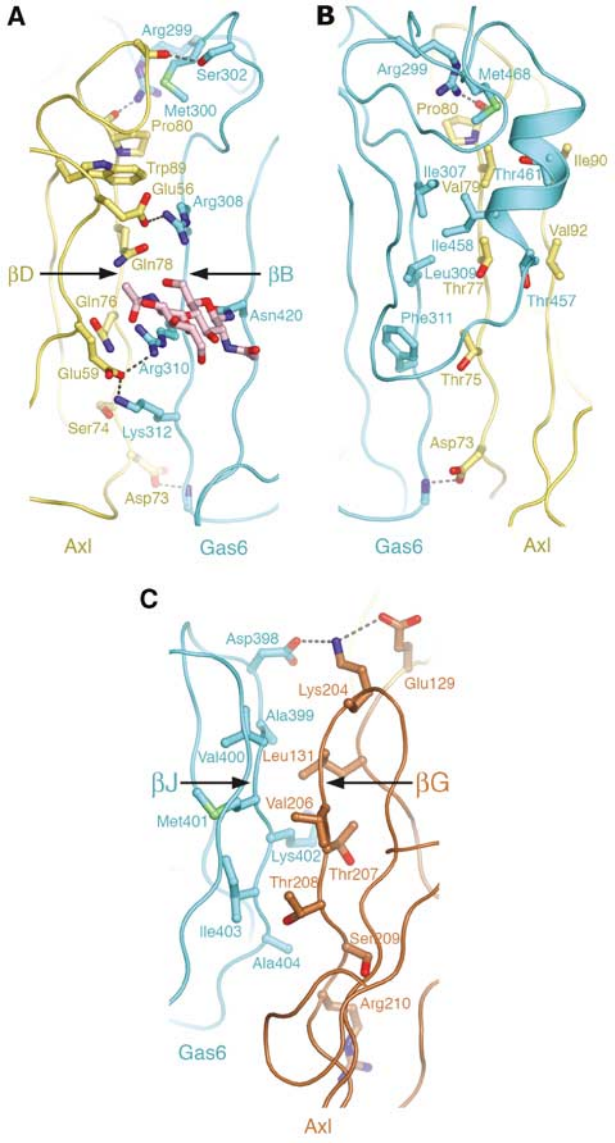

Figure 3 Detailed structure of the Gas6/Axl contact sites. (**A**) Front view of the major contact, in a direction similar to Figure 1C, showing the polar β-sheet surface. (**B**) Back view of the major contact, showing the apolar β-sheet surface. (**C**) Front view of the minor contact. Main chain traces are shown in the colours used in Figure 1. Selected interface residues are shown as sticks. The two N-acetylglucosamine moities attached to Asn420^{Gas6} are shown in pink. Hydrogen bonds are shown as broken lines. Main-chain hydrogen bonds between β-strands have been omitted for clarity.

Minor Gas6/Axl contact

The minor Gas6/Axl contact is formed between strands J of LG1^{Gas6} and strand G of IG2^{Axl}, with additional contributions from the domain linker of Axl-IG (Figure 3C). Apart from three main-chain hydrogen bonds, there is only one polar interaction in this region, between Asp398^{Gas6} and Lys204^{Axl}. Additionally, there are several van der Waals contacts that may impart specificity: most notably, Leu131^{Axl} is inserted into a pocket delineated by Ala399^{Gas6} and Lys402^{Gas6}, and the Cβ atom of Ala404^{Gas6} makes a close contact with Cα of Arg210^{Axl}.

Both Gas6/Axl contacts are required for receptor activation

As it is often difficult to distinguish crystal lattice contacts from genuine, physiological ligand/receptor interactions, we sought to confirm our interpretation of the Gas6-LG/Axl-IG structure by designing mutations that would disrupt specifically the major or minor contact in the 2:2 Gas6-LG/Axl-IG complex, or were predicted to have no effect (control mutations). The choice of mutations was complicated by the fact that both Gas6/Axl contacts prominently involve β-strand interactions, which are made by the polypeptide backbone and therefore not easily disrupted by mutagenesis.

Table I Mutational analysis of the Gas6/Axl interaction

Immobilised protein	Soluble protein	Location of mutation	$K_{0.5}$ (nM)[a]	K_d (nM)[b]
Axl-ex[c]	*Gas6-LG*		0.7	5±1
	T304D	Near major site	2	17±4
	R310E	Major site	>200	90±32
	K312E	Major site	>200	134±16
	R310E/K312E	Major site	>1000	4000±1000
	A404V	Minor site	0.7	18±5
	F485A	LG2 (control)	0.8	7±2
Axl-IG	*Gas6-LG*		1	6±2
Q54R		IG1 (control)	1.5	7±3
E56R		Major site	6	10±2
E59R		Major site	40	98±24
E56R/E59R		Major site	60	136±12
T77R		Major site	>200	311±118
Q122R		IG2 (control)	3	10±3
L131E		Minor site	1.5	9±4
K204E		Minor site	2	21±2
T208E		Minor site	2	21±4

[a]Concentration of soluble ligand at half-maximum binding in the solid-phase assay. The binding curves of several mutants did not reach saturation even at the highest concentration tested (100 nM); in these cases, lower limits are quoted.
[b]Dissociation constant obtained by nonlinear fitting (1:1 model) of association and dissociation curves obtained by surface plasmon resonance. Values are given as mean±standard deviation (n=4–7).
[c]Soluble Axl ectodomain expressed in 293 cells (Sasaki *et al*, 2002).

At the major contact, mutation of Glu59^{Axl} and Thr77^{Axl} dramatically reduced Gas6 binding both in a solid-phase assay and when measured by surface plasmon resonance (Table I). Likewise, mutation of Arg310^{Gas6} and Lys312^{Gas6} all but abolished Axl binding in both assays. Thus, the major contact in the Gas6-LG/Axl-IG complex indeed corresponds to the high-affinity interaction site. We were surprised that Glu56^{Axl} in the B-C loop of IG1^{Axl} does not seem to be required for a high-affinity interaction, given that this residue makes a specific electrostatic interaction with Gas6. However, Glu56^{Axl} remains partly exposed in the complex, and its role may be redundant (see below).

To test whether the major contact is required for Gas6–Axl signalling, we compared wild-type and mutant Gas6-LG proteins in a receptor activation assay, using a tumour cell line expressing Axl (Sasaki *et al*, 2002). Mutation of Arg310^{Gas6} and Lys312^{Gas6} reduced Axl phosphorylation to background levels (Figure 4), showing that the major Gas6/Axl contact is required for productive signalling. Unfortunately, the effect of Axl mutations on signalling could not be studied, since overexpression of Axl in a number of cell lines resulted in constitutive receptor activation in the absence of Gas6 (data not shown).

Mutation of Axl or Gas6 at the minor contact did not appreciably affected their high-affinity interaction, as

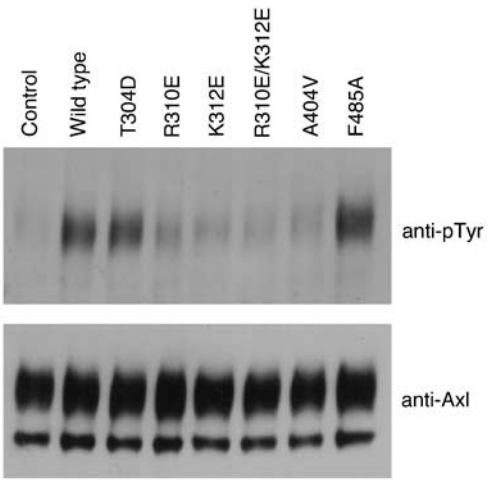

Figure 4 Axl activation by wild-type and mutant Gas6-LG. Human U-118 glioblastoma cells were incubated with 200 ng/ml Gas6-LG proteins for 15 min, the cells lysed, and the Axl receptor immunoprecipitated. Blots were probed with an anti-phosphotyrosine antibody, stripped, and reprobed with anti-Axl antiserum. The control experiment was carried out with no Gas6-LG protein added. The experiment was carried out three times with similar results.

expected (Table I). Crucially, however, mutation of $Ala404^{Gas6}$ resulted in a marked reduction of Axl activation (Figure 4). $Ala404^{Gas6}$ is fully exposed in free Gas6, but becomes partly buried at the minor contact in the complex. Thus, the reduced activity of the Gas6-LG A404V mutant demonstrates that the minor contact is functionally important and not a crystal lattice artefact. In support of this conclusion, a monoclonal antibody that partially blocks the Gas6/Axl interaction
recognises Gas6 residues 393–414, which contain the Axl-binding β-strand J and $Ala404^{Gas6}$ (Fisher *et al*, 2005). The combined data demonstrate that the 2:2 Gas6/Axl complex seen in our crystals represents a physiologically relevant assembly.

Sequence conservation of Gas6/receptor contacts

All Gas6 regions involved in Axl binding, including the glycosylation site at $Asn420^{Gas6}$ in the major contact, are strictly conserved in vertebrate Gas6 sequences (not shown). Comparing Axl with its family members Sky and Mer, we were surprised to find that only the minor Gas6 binding site in $IG2^{Axl}$ is highly conserved, whereas the major site in $IG1^{Axl}$ is not well conserved in Sky and Mer (Figure 2C). However, even though individual amino acids are not conserved, pertinent characteristics of the major Gas6 binding site in Axl appear to be conserved, at least in Sky (for which structural information is available; Heiring *et al*, 2004): the B-C loop of IG1 contains negatively charged residues, and strand D is quite long and features an unusually apolar surface that is contiguous with exposed apolar residues on strand E. The hydrophobic nature of the D-E surface is illustrated by the fact that, in the absence of Gas6, the Sky IG pair forms dimers in which the Gas6-binding D-E surface in IG1 is occluded in the dimer interface. This dimer may be an artefact of bacterial expression, since a putative glycosylation site is buried in the dimer interface (Figure 2C). Importantly, it has been shown that the dimer dissociates upon addition of Gas6-LG, resulting in the formation of a ligand/receptor complex with 1:1 stoichiometry (Heiring *et al*, 2004). Modelling shows that monomeric Sky is readily accommodated at the major Axl binding site of Gas6-LG (not shown).

With respect to the third Gas6 receptor, Mer, it is difficult to discern any conservation of Gas6 binding features at the major contact, and this may be correlated with the reduced affinity of Mer for Gas6 (Nagata *et al*, 1996). We cannot exclude that Mer (or, indeed, Sky) binds Gas6 in a different manner than Axl, but we think this is unlikely. It is also worth noting that all putative N-linked glycosylation sites in Sky and Mer (a total of seven sites, only one of which is shared with Axl) map to solvent-exposed positions in the Gas6-LG/Axl-IG structure. Given that all three Axl family receptors have multiple glycosylation sites within their IG domains (Figure 2C), the complete absence of such sites from the predicted Gas6 binding regions supports a conserved ligand-binding mode.

Discussion

RTK activation is believed to result from ligand-induced receptor dimerisation, leading to the autophosphorylation of multiple tyrosine residues in the cytosolic domains, and to downstream signalling (Schlessinger, 2000). Indeed, the close approximation of (at least) two receptors is a feature of all known structures of ligand/RTK complexes, but the mechanism by which receptor dimerisation is brought about is different in each case (Schlessinger, 2000; Wiesmann *et al*, 2000; Himanen *et al*, 2001; Burgess *et al*, 2003). Additional complexity is introduced by a variety of autoinhibitory mechanisms that help maintain RTKs in an inactive state in the absence of ligand, and the existence of (obligate) coreceptors. The architecture of the heterotetrameric Gas6/Axl complex described here most closely resembles that of the ephrin/Eph complex (Himanen *et al*, 2001), even though the two systems are completely different in their domain organisation. Both complexes are circular 2:2 assemblies with two distinct ligand/receptor interfaces of different affinity, and no direct ligand/ligand or receptor/receptor contacts. Like Eph signalling, Axl signalling is likely to be initiated by the formation of a high-affinity 1:1 ligand/receptor complex. Gas6/Axl complex formation may be driven initially by the combination of charge complementarity and hydrophobicity at the major contact site, followed by the receptor-induced freezing of mobile Gas6 regions. Lateral diffusion of 1:1 complexes would then lead to the formation of a minimal 2:2 Gas6/Axl signalling complex. Further aggregation of 2:2 complexes has been demonstrated to be required for Eph signalling (Smith *et al*, 2004). Whether Axl/Axl interactions contribute to signalling remains to be established.

The central role of hydrogen pairing between β-strands in both types of Gas6/Axl contacts is surprising, given that these interactions are not sequence-specific. At the major Gas6/Axl contact, the striking segregation of polar/ionic and apolar side chain interactions to opposite surfaces of the newly formed β-sheet appears to ensure the specific recognition of the cognate ligand. The precise nature of many of these interactions may be less critical, as suggested by the modest shape complementarity at this contact and the lack of sequence conservation of many Gas6 binding residues in

the other Axl family receptors, Sky and Mer. The minor Gas6/Axl contact is likely to be very weak and may owe its existence to the high cooperativity of forming a circular 2:2 complex. Nevertheless, the minor contact is critical for signal transduction, as suggested by its striking sequence conservation and experimentally verified by mutagenesis of $Ala404^{Gas6}$. Molecules that are able to inhibit Gas6/Axl signalling are potentially useful in controlling thrombosis (Angelillo-Scherrer *et al*, 2005; Gould *et al*, 2005), and our structure provides a framework for the rational design of such blocking agents. Targetting the Gas6/Axl contacts seen in our structure by small molecule antagonists may prove challenging, however: one contact is very large, and the other involves little more than the interaction of two solvent-exposed β-strands.

Several questions remain unanswered by our structure of a minimal Gas6/Axl complex. The Gla domain of Gas6 is dispensable for Axl activation in cultured cells, but its role *in vivo* has not been studied. The Gla domain may help recruit Gas6 to the cell surface harbouring its receptor. Model building shows that this is sterically feasible; the EGF-like domain preceding $LG1^{Gas6}$ could interact with the hydrophobic patch in $LG2^{Gas6}$, previously speculated to be involved in receptor binding (Sasaki *et al*, 2002). Alternatively, Gas6 could be bound to a different cell membrane than its receptor, similar to the ephrin/Eph situation. The physiological role, if any, of receptor dimerisation also remains to be studied. The fully glycosylated Axl ectodomain forms dimers with a dissociation constant of $\sim 10\,\mu M$ (our unpublished results), but whether this association occludes the major Gas6 binding site, as in the Sky structure (Heiring *et al*, 2004), is not known. To understand Gas6/Axl signalling in a cellular context, it will be important to determine the oligomeric state of Axl within the cell membrane and how it is affected by Gas6 binding. Our structure and mutational validation of a minimal Gas6/Axl complex has revealed the unique mechanism by which Axl family RTKs are dimerised by Gas6, and provides a solid basis to guide future investigations into this system.

Materials and methods

Protein production and mutagenesis

Human Gas6-LG was expressed in human embryonic kidney (293-EBNA) cells and purified as described (Sasaki *et al*, 2002). Point mutations were introduced by fusion PCR and confirmed by sequencing. All mutants behaved indistinguishable from wild-type Gas6-LG during purification. Soluble Axl-IG was expressed in *Escherichia coli* BL21 cells, by secretion into the periplasmic space. DNA coding for Axl residues 26–220 (sequence numbering includes the signal peptide as defined in SwissProt entry P30530) was obtained by PCR from a full-length human Axl cDNA and cloned into pASK-IBA12 (N-terminal Strept-tag II) or pASK-IBA32 (C-terminal His-tag) (IBA GmbH, Göttingen, Germany). Point mutations were introduced using a site-directed mutagenesis kit (Stratagene, CA, USA) and confirmed by sequencing. Proteins were purified according to the manufacturer's instructions. The Strept-tag was removed by thrombin digestion. The untagged Axl-IG was purified by gel filtration (Superose 12 HR 16/50) and mixed with Gas6-LG in a 1:1 molar ratio. The resulting Gas6-LG/Axl-IG complex was purified by gel filtration prior to crystallisation.

Binding and activation assays

The solid-phase assay and surface plasmon resonance experiments were carried out as described previously (Sasaki *et al*, 2002). Soluble Axl ectodomain (Sasaki *et al*, 2002) or Axl IG1–2 and its mutants (His-tagged proteins) were immobilised, and Gas6-LG and its mutants were used as soluble ligands. Axl activation by wild-type and mutant Gas6-LG in human U-118 glioblastoma cells was also carried out as described previously (Sasaki *et al*, 2002).

Table II Crystallographic statistics

Data collection and reduction	
Space group	$P6_1$
Unit cell dimensions	$a = b = 292.95$ Å, $c = 63.95$ Å
Resolution range (Å)	20.0 (3.48)–3.3
Unique reflections	47 655
Multiplicity	5.9 (5.8)
Completeness (%)	99.5 (100)
Mean I/σ (I)	11.3 (3.7)
R_{merge}	0.118 (0.432)
Refinement	
Reflections (working set/test set)	45 264/2384
Atoms	8903
R_{cryst}/R_{free}	0.241/0.265
R.m.s. deviations	
Bond lengths (Å)	0.009
Bond angles (deg)	1.5
B-factors (Å^2)	1.9
NCS (Å)[a]	0.20
Ramachandran plot (%)[b]	74.5/23.2/2.3/0

Numbers in parantheses refer to data in the highest resolution shell.
[a]Deviation between the two crystallographically independent Gas6-LG/Axl-IG copies (571 Cα atoms).
[b]Residues in most favoured, additionally allowed, generously allowed, and disallowed regions (Laskowski *et al*, 1993).

Crystal structure determination

For crystallisation, the Gas6-LG/Axl-IG complex was concentrated to 10 mg/ml in 0.025 M Na-HEPES pH 7.5, 0.15 M NaCl, 1 mM calcium acetate. Needle-shaped crystals were obtained at room temperature by the hanging drop method, using 0.1 M Tris–HCl pH 8.5, 0.6–0.8 M Li_2SO_4, 2 mM $NiSO_4$ as precipitant. The crystals were flash-frozen in mother liquour supplemented with 30% glycerol. X-ray diffraction data were collected at 100 K on beamline ID23-1 at the ESRF (Grenoble, France) using a Marmosaic 225 CCD detector ($\lambda = 0.9794$ Å). The crystals diffracted extremely weakly and data were collected using an unattenuated beam and 20 s exposures per 0.5° frame. There are two copies of a 1:1 Gas6-LG/Axl-IG complex in the asymmetric unit of the hexagonal crystals, related by a noncrystallographic two-fold symmetry axis perpendicular to the crystallographic six-fold axis. The solvent content of the crystals is unusually high at 78%, explaining the weak diffraction. The diffraction data were processed with MOSFLM (http://www.mrc-lmb.cam.ac.uk/harry/mosflm/) and programs of the CCP4 suite (CCP4-Collaborative Computing Project No. 4, 1994). The structure was solved by molecular replacement with PHASER (Storoni *et al*, 2004), using the Gas6-LG (Sasaki *et al*, 2002) and Sky-IG (Heiring *et al*, 2004) structures as search models; the IG domains of Sky had to be placed individually to obtain a solution. The structure was rebuilt with O (Jones *et al*, 1991) and refined with CNS (Brunger *et al*, 1998), using tight noncrystallographic symmetry restraints. The final model includes: Gas6 residues 279–493, 504–541, and 550–676, with two N-acetylglucosamine moieties attached to $Asn420^{Gas6}$; Axl residues 27–217; two calcium ions, two nickel ions, and one sulfate ion. Data collection and refinement statistics are summarised in Table II. Solvent-accessible areas were calculated with the CCP4 program AREAIMOL. The figures were made with PYMOL (http://www.pymol.org).

Supplementary data

Supplementary data are available at *The EMBO Journal* Online.

Acknowledgements

We thank Jürgen Engel and Ariel Lustig (Biozentrum Basel, Switzerland) for the analytical ultracentrifugation experiments;

Xavier Thibault and the staff at ESRF (Grenoble, France) and Federico Carafoli for help with X-ray data collection; Peter Brick, Jason Howitt and Birgit Leitinger for critical reading of the manuscript. This work was supported by a Wellcome Senior Research Fellowship to EH (ref 54334) and a DFG grant to RT (ref Ti95/8-2).

Accession code
The coordinates and structure factors of the Gas6-LG/Axl-IG complex have been deposited in the Protein Data Bank (accession code 2c5d).

References

Angelillo-Scherrer A, Burnier L, Flores N, Savi P, DeMol M, Schaeffer P, Herbert JM, Lemke G, Goff SP, Matsushima GK, Earp HS, Vesin C, Hoylaerts MF, Plaisance S, Collen D, Conway EM, Wehrle-Haller B, Carmeliet P (2005) Role of Gas6 receptors in platelet signaling during thrombus stabilization and implications for antithrombotic therapy. *J Clin Invest* **115:** 237–246

Angelillo-Scherrer A, de Frutos P, Aparicio C, Melis E, Savi P, Lupu F, Arnout J, Dewerchin M, Hoylaerts M, Herbert J, Collen D, Dahlback B, Carmeliet P (2001) Deficiency or inhibition of Gas6 causes platelet dysfunction and protects mice against thrombosis. *Nat Med* **7:** 215–221

Brunger AT, Adams PD, Clore GM, DeLano WL, Gros P, Grosse-Kunstleve RW, Jiang JS, Kuszewski J, Nilges M, Pannu NS, Read RJ, Rice LM, Simonson T, Warren GL (1998) Crystallography & NMR system: a new software suite for macromolecular structure determination. *Acta Crystallogr D Biol Crystallogr* **54:** 905–921

Burgess AW, Cho HS, Eigenbrot C, Ferguson KM, Garrett TP, Leahy DJ, Lemmon MA, Sliwkowski MX, Ward CW, Yokoyama S (2003) An open-and-shut case? Recent insights into the activation of EGF/ErbB receptors. *Mol Cell* **12:** 541–552

Casasnovas JM, Stehle T, Liu JH, Wang JH, Springer TA (1998) A dimeric crystal structure for the N-terminal two domains of intercellular adhesion molecule-1. *Proc Natl Acad Sci USA* **95:** 4134–4139

CCP4-Collaborative Computing Project No 4 (1994) The CCP4 suite: programs for protein crystallography. *Acta Crystallogr D Biol Crystallogr* **50:** 760–763

Chothia C, Jones EY (1997) The molecular structure of cell adhesion molecules. *Annu Rev Biochem* **66:** 823–862

Fisher PW, Brigham-Burke M, Wu SJ, Luo J, Carton J, Staquet K, Gao W, Jackson S, Bethea D, Chen C, Hu B, Giles-Komar J, Yang J (2005) A novel site contributing to growth-arrest-specific gene 6 binding to its receptors as revealed by a human monoclonal antibody. *Biochem J* **387:** 727–735

Godowski PJ, Mark MR, Chen J, Sadick MD, Raab H, Hammonds RG (1995) Reevaluation of the roles of protein S and Gas6 as ligands for the receptor tyrosine kinase Rse/Tyro 3. *Cell* **82:** 355–358

Goruppi S, Ruaro E, Schneider C (1996) Gas6, the ligand of Axl tyrosine kinase receptor, has mitogenic and survival activities for serum starved NIH3T3 fibroblasts. *Oncogene* **12:** 471–480

Gould WR, Baxi SM, Schroeder R, Peng YW, Leadley RJ, Peterson JT, Perrin LA (2005) Gas6 receptors Axl, Sky and Mer enhance platelet activation and regulate thrombotic responses. *J Thromb Haemost* **3:** 733–741

Gschwind A, Fischer OM, Ullrich A (2004) The discovery of receptor tyrosine kinases: targets for cancer therapy. *Nat Rev Cancer* **4:** 361–370

Heiring C, Dahlback B, Muller YA (2004) Ligand recognition and homophilic interactions in Tyro3: structural insights into the Axl/Tyro3 receptor tyrosine kinase family. *J Biol Chem* **279:** 6952–6958

Himanen JP, Rajashankar KR, Lackmann M, Cowan CA, Henkemeyer M, Nikolov DB (2001) Crystal structure of an Eph receptor-ephrin complex. *Nature* **414:** 933–938

Janssen JW, Schulz AS, Steenvoorden AC, Schmidberger M, Strehl S, Ambros PF, Bartram CR (1991) A novel putative tyrosine kinase receptor with oncogenic potential. *Oncogene* **6:** 2113–2120

Jones TA, Zhou JY, Cowan SW, Kjeldgaard M (1991) Improved methods for building protein models in electron density maps and the location of errors in these models. *Acta Crystallogr A* **47:** 110–119

Laskowski RA, MacArthur MW, Moss DS, Thornton JM (1993) PROCHECK: a program to check the stereochemical quality of protein structures. *J Appl Crystallogr* **26:** 283–291

Li R, Chen J, Hammonds G, Phillips H, Armanini M, Wood P, Bunge R, Godowski PJ, Sliwkowski MX, Mather JP (1996) Identification of Gas6 as a growth factor for human Schwann cells. *J Neurosci* **16:** 2012–2019

Lu Q, Gore M, Zhang Q, Camenisch T, Boast S, Casagranda F, Lai C, Skinner MK, Klein R, Matsushima GK, Earp HS, Goff SP, Lemke G (1999) Tyro-3 family receptors are essential regulators of mammalian spermatogenesis. *Nature* **398:** 723–728

Lu Q, Lemke G (2001) Homeostatic regulation of the immune system by receptor tyrosine kinases of the Tyro 3 family. *Science* **293:** 306–311

Manfioletti G, Brancolini C, Avanzi G, Schneider C (1993) The protein encoded by a growth arrest-specific gene (gas6) is a new member of the vitamin K-dependent proteins related to protein S, a negative coregulator in the blood coagulation cascade. *Mol Cell Biol* **13:** 4976–4985

Mark MR, Chen J, Hammonds RG, Sadick M, Godowski PJ (1996) Characterization of Gas6, a member of the superfamily of G domain-containing proteins, as a ligand for Rse and Axl. *J Biol Chem* **271:** 9785–9789

Nagata K, Ohashi K, Nakano T, Arita H, Zong C, Hanafusa H, Mizuno K (1996) Identification of the product of growth arrest-specific gene 6 as a common ligand for Axl, Sky, and Mer receptor tyrosine kinases. *J Biol Chem* **271:** 30022–30027

Nakano T, Higashino K, Kikuchi N, Kishino J, Nomura K, Fujita H, Ohara O, Arita H (1995) Vascular smooth muscle cell-derived, Gla-containing growth-potentiating factor for Ca(2+)-mobilizing growth factors. *J Biol Chem* **270:** 5702–5705

Nakano T, Tani M, Ishibashi Y, Kimura K, Park YB, Imaizumi N, Tsuda H, Aoyagi K, Sasaki H, Ohwada S, Yokota J (2003) Biological properties and gene expression associated with metastatic potential of human osteosarcoma. *Clin Exp Metastasis* **20:** 665–674

O'Bryan JP, Frye RA, Cogswell PC, Neubauer A, Kitch B, Prokop C, Espinosa III R, Le Beau MM, Earp HS, Liu ET (1991) axl, a transforming gene isolated from primary human myeloid leukemia cells, encodes a novel receptor tyrosine kinase. *Mol Cell Biol* **11:** 5016–5031

O'Donnell K, Harkes IC, Dougherty L, Wicks IP (1999) Expression of receptor tyrosine kinase Axl and its ligand Gas6 in rheumatoid arthritis: evidence for a novel endothelial cell survival pathway. *Am J Pathol* **154:** 1171–1180

Ohashi K, Nagata K, Toshima J, Nakano T, Arita H, Tsuda H, Suzuki K, Mizuno K (1995) Stimulation of sky receptor tyrosine kinase by the product of growth arrest-specific gene 6. *J Biol Chem* **270:** 22681–22684

Rescigno J, Mansukhani A, Basilico C (1991) A putative receptor tyrosine kinase with unique structural topology. *Oncogene* **6:** 1909–1913

Sasaki T, Knyazev PG, Cheburkin Y, Gohring W, Tisi D, Ullrich A, Timpl R, Hohenester E (2002) Crystal structure of a C-terminal fragment of growth arrest-specific protein Gas6. Receptor tyrosine kinase activation by laminin G-like domains. *J Biol Chem* **277:** 44164–44170

Schlessinger J (2000) Cell signaling by receptor tyrosine kinases. *Cell* **103:** 211–225

Scott RS, McMahon EJ, Pop SM, Reap EA, Caricchio R, Cohen PL, Earp HS, Matsushima GK (2001) Phagocytosis and clearance of apoptotic cells is mediated by MER. *Nature* **411:** 207–211

Shankar SL, O'Guin K, Cammer M, McMorris FA, Stitt TN, Basch RS, Varnum B, Shafit-Zagardo B (2003) The growth arrest-specific gene product Gas6 promotes the survival of human oligodendrocytes via a phosphatidylinositol 3-kinase-dependent pathway. *J Neurosci* **23:** 4208–4218

Smith FM, Vearing C, Lackmann M, Treutlein H, Himanen J, Chen K, Saul A, Nikolov D, Boyd AW (2004) Dissecting the EphA3/

Ephrin-A5 interactions using a novel functional mutagenesis screen. *J Biol Chem* **279:** 9522–9531

Stitt TN, Conn G, Goret M, Lai C, Bruno J, Radzlejewski C, Mattsson K, Fisher J, Gies DR, Jones PF, Masiakowski P, Ryan TE, Tobkes NJ, Chen DH, DiStefano PS, Long GL, Basilico C, Goldfarb MP, Lemke G, Glass DJ, Yancopoulos GD (1995) The anticoagulation factor protein S and its relative, Gas6, are ligands for the Tyro 3/Axl family of receptor tyrosine kinases. *Cell* **80:** 661–670

Storoni LC, McCoy AJ, Read RJ (2004) Likelihood-enhanced fast rotation functions. *Acta Crystallogr D Biol Crystallogr* **60:** 432–438

Sun W, Fujimoto J, Tamaya T (2004) Coexpression of Gas6/Axl in human ovarian cancers. *Oncology* **66:** 450–457

Tanabe K, Nagata K, Ohashi K, Nakano T, Arita H, Mizuno K (1997) Roles of gamma-carboxylation and a sex hormone-binding globulin-like domain in receptor-binding and in biological activities of Gas6. *FEBS Lett* **408:** 306–310

Tisi D, Talts JF, Timpl R, Hohenester E (2000) Structure of the C-terminal laminin G-like domain pair of the laminin alpha2 chain harbouring binding sites for alpha-dystroglycan and heparin. *EMBO J* **19:** 1432–1440

Varnum BC, Young C, Elliott G, Garcia A, Bartley TD, Fridell Y, Hunt RW, Trail G, Clogston C, Toso RJ, Yanagihara D, Bennett L, Sylber M, Merewether LA, Tseng A, Escobar E, Liu ET, Yamane HK (1995) Axl receptor tyrosine kinase stimulated by the vitamin K-dependent protein encoded by growth-arrest-specific gene 6. *Nature* **373:** 623–626

Wiesmann C, Muller YA, de Vos AM (2000) Ligand-binding sites in Ig-like domains of receptor tyrosine kinases. *J Mol Med* **78:** 247–260

Yanagita M, Ishimoto Y, Arai H, Nagai K, Ito T, Nakano T, Salant DJ, Fukatsu A, Doi T, Kita T (2002) Essential role of Gas6 for glomerular injury in nephrotoxic nephritis. *J Clin Invest* **110:** 239–246